

Long-range spatial correlations in the exciton energy distribution in GaAs/AlGaAs quantum-wells

Y. Yayon, A. Esser^(*), M. Rappaport, V. Umansky, H. Shtrikman and I. Bar-Joseph
Departement of Condensed Matter Physics, The Weizmann Institute of Science, Rehovot 76100, Israel
^(*) *AG Halbleitertechnik, Institut für Physik, Humboldt University Berlin, Germany*

Variations in the width of a quantum well (QW) are known to be a source of broadening of the exciton line. Using low temperature near-field optical microscopy, we have exploited the dependence of exciton energy on well-width to show that in GaAs QWs, these seemingly random well-width fluctuations actually exhibit well-defined order — strong long-range correlations appearing laterally, in the plane of the QW, as well as vertically, between QWs grown one on top of the other. We show that these fluctuations are correlated with the commonly found mound structure on the surface. This is an intrinsic property of molecular beam epitaxial growth.

PACS:

The confinement of electrons and holes to two dimensions (2D) in semiconductor quantum wells (QWs) alters the density of states and interactions, making them an ideal system for studying 2D physics. It is well known that QW interfaces are not perfect, and some roughness, which depends on the growth conditions, is always present. As a result, the QW width is not uniform and the confinement energy fluctuates in the plane. This gives rise to a disorder potential, which strongly affects the behavior of particles and quasi-particles in the QW.

This interface disorder potential plays a particularly dominant role in determining the behavior of QW excitons. These objects are localized in this potential and their energy spectrum becomes discrete. Indeed, exciton localization in this disordered system has been a subject of intense theoretical research, and a variety of spectroscopic techniques were implemented to study its manifestation in the optical spectrum. Important insight into this problem came with the application of scanning near-field optical microscopy (SNOM) to the study of QW photoluminescence (PL). In a pioneering work, Hess *et al.* have directly shown that the far-field inhomogeneously broadened line of the exciton splits into many narrow lines in the near-field, each line corresponding to a different exciton eigenstate of the disordered potential [1]. This work was followed by a number of SNOM measurements that investigated the local properties of excitons in the spatially fluctuating potential of a QW [2–6]. A considerable attention was recently directed to the statistical properties of the exciton energy levels in this system [6,7]. It was shown that the exciton energy levels in a disordered narrow QW are not randomly spaced but rather exhibit 'level repulsion' behavior, manifested by a characteristic spacing between the energies.

The common assumption in the theoretical studies of exciton localization in QWs is a disorder potential with only a single short-range correlation length ξ , which is of the order of the exciton Bohr radius a_B [8]. Indeed, previous near-field measurements have focused on narrow (~ 3 nm) QWs in which single localized excitons can be resolved and direct insight into the short-range correlations (e.g., extended states, level repulsion) is obtained [2,6]. In this work we focus on broad QWs (10–20 nm) in which the short-range behavior is averaged by the SNOM tip, and we study in detail the vertical and lateral long-range order of the exciton energy distribution. We find that the seemingly random exciton energy fluctuations exhibit well defined order: strong long-range correlations appear both laterally, in the plane of the QW, and vertically, between QWs grown one above the other. We show that this behavior is general and stems from an intrinsic property of molecular beam epitaxial (MBE) growth.

The measurements presented in this work were performed on three GaAs QW samples. Samples 1 and 2 are modulation-doped and have similar structures: They both have a single 20 nm GaAs QW. In sample 1 a 3.6 nm Si-doped donor layer is separated from the QW by a 50 nm $\text{Al}_{0.35}\text{Ga}_{0.65}\text{As}$ spacer layer and the distance between the QW and the sample surface is 96 nm. In sample 2 the Si-doped layer has a width of 15 nm, and the spacer is a 60 nm layer of $\text{Al}_{0.35}\text{Ga}_{0.65}\text{As}$. The distance between the QW and the sample surface is 63 nm. In both samples a $2 \times 2 \text{ mm}^2$ mesa was etched, and ohmic contacts were alloyed to the QW layer. A 4.5 nm PdAu semitransparent gate was evaporated on top of the samples. All the data were taken at a gate voltage such that the QW is depleted of electrons and the PL spectrum is dominated by the neutral exciton transition. Sample 3 consists of four QWs of widths 25, 17, 11 and 5 nm, grown in that order and separated from each other by 20 nm AlAs layers. The uppermost QW (5 nm) is 50 nm below the sample surface. The overall growth thickness in samples 1, 2, and 3 are 1.57 μm , 1.11 μm , and 1.23 μm , respectively.

The local measurement of the PL spectrum is performed with a homemade SNOM operating at 4.2 K [9]. The sample is illuminated uniformly by a single-mode fiber and the emitted PL is collected through a tapered Au-coated etched optical fiber tip [10]. The tip collects the PL and guides it through an optical fiber into a spectrometer, where it is dispersed onto a liquid nitrogen cooled CCD camera. The overall spectral resolution is 80 μeV . The spatial resolution is determined by the tip diameter. We have conducted measurements with tips of

various diameters in the range of $0.2 - 0.3 \mu\text{m}$.

We begin by studying the lateral distribution of the exciton peak energy E_X in the two single QW samples. Figures 1a and 1b are mappings of E_X in the two samples, each over an area of $11 \times 11 \mu\text{m}^2$ (111×111 points). The images are color coded from dark to bright, corresponding to low and high exciton energies, respectively. The near-field exciton lineshape in both samples is found to be Gaussian throughout the measured area, with typical full widths at half maxima of $\sim 0.5 \text{ meV}$. The peak of the Gaussian fit allowed E_X to be extracted with an accuracy which is better than our spectral resolution. The near-field Gaussian lineshape indicates the existence of inhomogeneous broadening on the tip-size scale. The near-field spectrum is therefore a superposition of many exciton lines, localized in the short-range fluctuations, on a scale smaller than the tip size.

The two images seem random, with no apparent order in the energy distribution. It is seen that there is clear distinction between the two: in sample 1, E_X varies on a significantly shorter length scale than in sample 2. Examining the fluctuation amplitude another difference is noticeable: in sample 1 the mean fluctuation is $\sim 0.1 \text{ meV}$, significantly smaller than the typical near-field inhomogeneous line-width of the exciton, whereas in sample 2 it is $\sim 0.4 \text{ meV}$, comparable to the inhomogeneous width. To examine the presence of underlying long-range order and spatial correlations in these seemingly random energy distributions we calculated the 2D autocorrelation function, defined as

$$G_X(x, y) = \langle E(x', y') E(x' - x, y' - y) \rangle. \quad (1)$$

Here $\langle \dots \rangle$ denotes averaging over all measured points in the scanned area, and $E(x, y) = E_X(x, y) - \langle E_X(x, y) \rangle$. The correlation function averages out the random behavior and highlights the correlated part of the signal. In particular, periodic peaks in $G_X(x, y)$ indicate the existence of periodicity in the exciton energy distribution. Figures 1c and 1d show plots of $G_X(x, y)$ for the data of Figs. 1a and 1b, respectively. The plots are color coded such that bright and dark regions correspond to strong and weak correlations (large and small G_X), respectively. Clear symmetry axes and periodicity are observed in both figures. It is seen that the maxima of $G_X(x, y)$ in both figures are arranged along lines that match the $[100]$ and $[010]$ crystallographic orientations [11]. Furthermore, these maxima exhibit a periodicity of ~ 1.8 in sample 1 and $\sim 3 \mu\text{m}$ in sample 2. In fact, it is seen that the peaks form a structure that resembles a *cubic lattice*.

The existence of this surprising long-range order along crystallographic directions clearly indicates that its origin is the structure of the GaAs/AlGaAs crystal. To understand the relationship between the exciton energy fluctuations and the crystalline structure we have used the SNOM to examine the topography of the sample surface $h(x, y)$. We note that the topography provides us with a

measure of the *integrated* evolution of the GaAs/AlGaAs crystal following a growth of $\sim 1 \mu\text{m}$, while the exciton energy, which is related to the local well width, gives the *differential* behavior over 20 nm at the final stage of the growth. Since the topography is measured in the SNOM simultaneously with the near-field spectra, one obtains the two signals, $E_X(x, y)$ and $h(x, y)$, at exactly the same location. We find that the samples' surface is covered with mounds with a typical height of 10 nm (Fig. 2a and 2b). Comparing the force images to the exciton energy images, one can clearly see the similarity between them. In Figs. 2c and 2d we show the autocorrelation function $G_h(x, y)$ of the topography images for the same areas as in Figs. 1c and 1d. We can see that the surface topography also exhibits long-range order, which is similar to that of E_X . The similarity between $G_X(x, y)$ and $G_h(x, y)$ is especially pronounced in sample 2, where the two functions exhibit the same symmetry and periodicity. This is demonstrated in Fig. 3, which shows a cut through the origin of both functions along the $[010]$ direction. Remarkably, the periodicity is exactly the same for the two lines.

The formation of mounds on surfaces of MBE-grown samples has been a subject of intensive study during the last decade. However, to the best of our knowledge, there is no detailed investigation of their influence on the QW width fluctuations. An important milestone was the finding that their origin is an intrinsic growth instability, which inhibits downward movement of adatoms at step edges [12,13]. It was shown that the mounds acquire an elongated shape in the $[1\bar{1}0]$ direction due to surface reconstruction of the As atoms, which terminate the As-rich (001) surface [14]. This anisotropy in the mounds' shape is clearly seen in the topography image of sample 1 (Fig. 2a). As more layers are added the mounds grow in height and a process of coarsening sets in, in which small mounds merge with larger ones, and the surface becomes completely covered with large mounds with a characteristic size and inclination angle [12]. The strong similarity between the long-range behavior of the exciton energy and the surface topography clearly indicates that the mound formation plays a dominant role in determining the QW width fluctuations. In particular, we believe that the coarsening process of the mound topography is responsible for the quasi-periodic structure that is observed both in the surface topography and exciton energy. It should be noted, however, that the exciton image in sample 1 does not show the anisotropy exhibited by the topography image. This is probably since the difference in growth along the two crystal directions is not significant for a thickness of 20 nm .

The notion that mound formation creates long-range correlations in the QW width fluctuations implies that there should be correlation in the vertical direction as well. To investigate this issue we have measured the near-field exciton energies of sample 3, which consists of four different QW grown one on top of the other. The spectral window of our spectrometer and CCD system enabled us

to measure simultaneously the spectra of three QWs (11, 17 and 25 nm), thus, avoiding any drift that could occur in sequential measurements. In Fig. 4a we show the fluctuations in the exciton energies of the three QWs along an 11 μm line. The near-field exciton lineshapes of the two narrower wells were non-Gaussian, consisting of multiple peaks. To determine the characteristic exciton energy, $E_X(x, y)$, for each location we calculated the energy center-of-mass of each spectrum. This procedure enabled us to get very good accuracy for E_X . It is evident that there is an almost perfect correlation between the fluctuation patterns in the three QWs, indicating that they arise from the same physical origin. It is seen that this matching in the fluctuation patterns occurs down to sub-micron length scales. Indeed, we found that the topography of that sample is characterized by shallow and densely packed mounds. We note that the amplitude of the energy fluctuations increases as the well width decreases as expected. On the other hand, the bulk GaAs exciton peak, which is measured simultaneously in the same sample, shows much smaller fluctuations that are uncorrelated with those of the QWs peaks. This is a reassuring evidence that the observed fluctuations in the center-of-mass spectrum are indeed due to well width fluctuations. One can thus conclude that the process of mound formation indeed creates a strong vertical correlation between the width fluctuations of QWs grown one on top of the other.

The existence of this vertical correlation has significant implications for the understanding of the resonant Rayleigh scattering (RRS) in multiple QWs samples. It was recently shown that the RRS in multiple QWs is characterized by temporal oscillations, which are absent in single QW samples [15,16]. These oscillations were explained as resulting from exciton-polariton effects. However, in presenting this explanation it was implicitly assumed that full vertical correlation exists between the disorder in the QWs [15]. In fact, recent theoretical calculations have shown that these polaritonic effects depend critically on the amount of vertical correlation of the disorder between the wells, and disappear when only moderate correlation exists [8]. Our measurements provide direct evidence to the validity of that assumption, and substantiate the existence of strong vertical correlation.

We can now quantitatively analyze the relation between the characteristic amplitude of well-width fluctuations ΔL and the QW width L . Clearly, ΔL can be directly obtained from the amplitude of the exciton energy fluctuation, ΔE , and the mean energy, E_{QW} : for a QW with infinite barriers the relation is simply $\Delta E/E_{QW} = -2\Delta L/L$, and for finite barriers it can be calculated numerically. In Fig. 4b we rescale the data of Fig. 4a with the vertical scale being ΔL . Remarkably, the order of the lines has been changed and the largest fluctuations in well width are found in the widest well. To further establish this surprising conclusion we measured the exciton energy of the four quantum wells along

six lines, 11 μm long (corresponding to 666 measurement points), and calculated the standard-deviation, σ , of ΔL in each QW. In Fig. 5 we plot σ as a function of the QW width L . It is clearly seen that σ increases monotonically with L . One can thus conclude that the long-range part of the *well-width fluctuations increases with the well-width*. The mechanism that gives rise to this behavior is illustrated schematically in the inset of Fig. 5. The drawing shows the AlAs/GaAs and GaAs/AlAs interfaces for wide and narrow QWs. The coarsening process (discussed above) and the process of smoothening of the AlAs interface by the GaAs layers give rise to non-uniform growth of the quantum well. The well is thicker at the mounds minima and thinner at their maxima. As depicted in the drawing, the amplitude of the well width fluctuations, which is given by the difference between the wide and narrow regions, increases with the well width. To verify the correctness of this model we studied the local relation between $h(x, y)$ and $E_X(x, y)$ in all samples. A detailed examination of the topography and energy images reveals that at points where h is high E_X is also high, and vice versa. In other words, the well is *narrow* at places where the surface is high and *wide* where it is low.

In conclusion, we wish to note that the role of surface mounds in determining the spatial distribution of electrons in MBE-grown samples was recently realized [17,18]. Our work shows that this intrinsic property of MBE growth has far reaching effect on the optical spectrum of excitons in semiconductor QWs as well.

We are pleased to acknowledge the assistance of V. Zhuk in preparing the SNOM tips. The research was partially supported by the Israeli Science Foundation and the Minerva Foundation. A. Esser wishes to acknowledge the support of LSF grant (HPRI-CT-1999-00069).

Fig. 1: (a), (b) Two-dimensional images of the exciton energy, $E_X(x, y)$, for samples 1 and 2, respectively. The energy ranges in (a) and (b) are 0.2 and 0.5 meV, respectively. (c), (d) The autocorrelation function $G_X(x, y)$ for the range $-10 \mu\text{m} \leq x, y \leq 10 \mu\text{m}$, of the exciton images of samples 1 and 2, respectively.

Fig. 2: (a), (b) Surface topography images of samples 1 and 2, respectively. The full range is 20 nm. (c), (d) The autocorrelation function $G_h(x, y)$ for the range $-10 \mu\text{m} \leq x, y \leq 10 \mu\text{m}$, of the topography images of sample 1 and 2, respectively.

Fig. 3: Cuts through the origin of G_X and G_h along the [010] crystallographic orientation of sample 2.

Fig. 4: (a) The exciton energy fluctuations of three QWs grown one on top of the other along an 11 μm line. (b) The same line scan as in (a) translated to well-width fluctuations.

Fig. 5: The standard-deviation of the well-width fluctuations as a function of the well width. The inset shows a schematic drawing of the layers structure for narrow and wide QWs. Grey and white areas represent GaAs and AlGaAs layers, respectively.

-
- [1] H. F. Hess, *et al.*, Science, **264**, 1740 (1994).
 - [2] D. Gammon *et al.*, Phys. Rev. Lett. **76**, 3005 (1996).
 - [3] G. Eytan *et al.*, Phys. Rev. Lett. **81**, 1666 (1998).
 - [4] Q. Wu *et al.*, Phys. Rev. Lett. **83**, 2652 (1999).
 - [5] G. von Freymann *et al.*, Appl. Phys. Lett. **77**, 394 (2000).
 - [6] F. Intonti *et al.*, Phys. Rev. Lett. **87**, 076801 (2001).
 - [7] V. Savona and R. Zimmermann, Phys. Rev. B **60** 4928 (1999).
 - [8] R. Zimmermann, E. Runge and V. Savona, in "Quantum coherence, Correlation and decoherence in semiconductor nanostructures", Ed. T. Takagahara, Academic Press, to be published.
 - [9] G. Eytan *et al.*, Ultramicroscopy **83**, 25 (2000).
 - [10] P. Hoffmann *et al.*, Ultramicroscopy, **61**, 165 (1995).
 - [11] The $[1\bar{1}0]$ direction was determined by the "bowtie" defects on the back of the sample.
 - [12] C. Orme *et al.*, Appl. Phys. Lett. **64**, 860 (1994).
 - [13] M. D. Johnson *et al.*, Phys. Rev. Lett. **72**, 116 (1994).
 - [14] The dangling bonds of these atoms form dimers that are arranged in rows along the $[1\bar{1}0]$ direction, along which the growth rate is faster.
 - [15] G. Malpuech *et al.*, Phys. Rev. Lett. **85**, 650 (2000).
 - [16] J. P. Prineas *et al.*, Phys. Rev. Lett. **85**, 3041 (2000).
 - [17] R. L. Willett *et al.*, Phys. Rev. Lett. **87**, 126803 (2001).
 - [18] Y. Yayon *et al.*, to be published in Phys. Rev. B, 15 July (2002)

This figure "fig1.jpg" is available in "jpg" format from:

<http://arxiv.org/ps/cond-mat/0206431v1>

This figure "fig2.jpg" is available in "jpg" format from:

<http://arxiv.org/ps/cond-mat/0206431v1>

Fig. 3 Yayon et al.

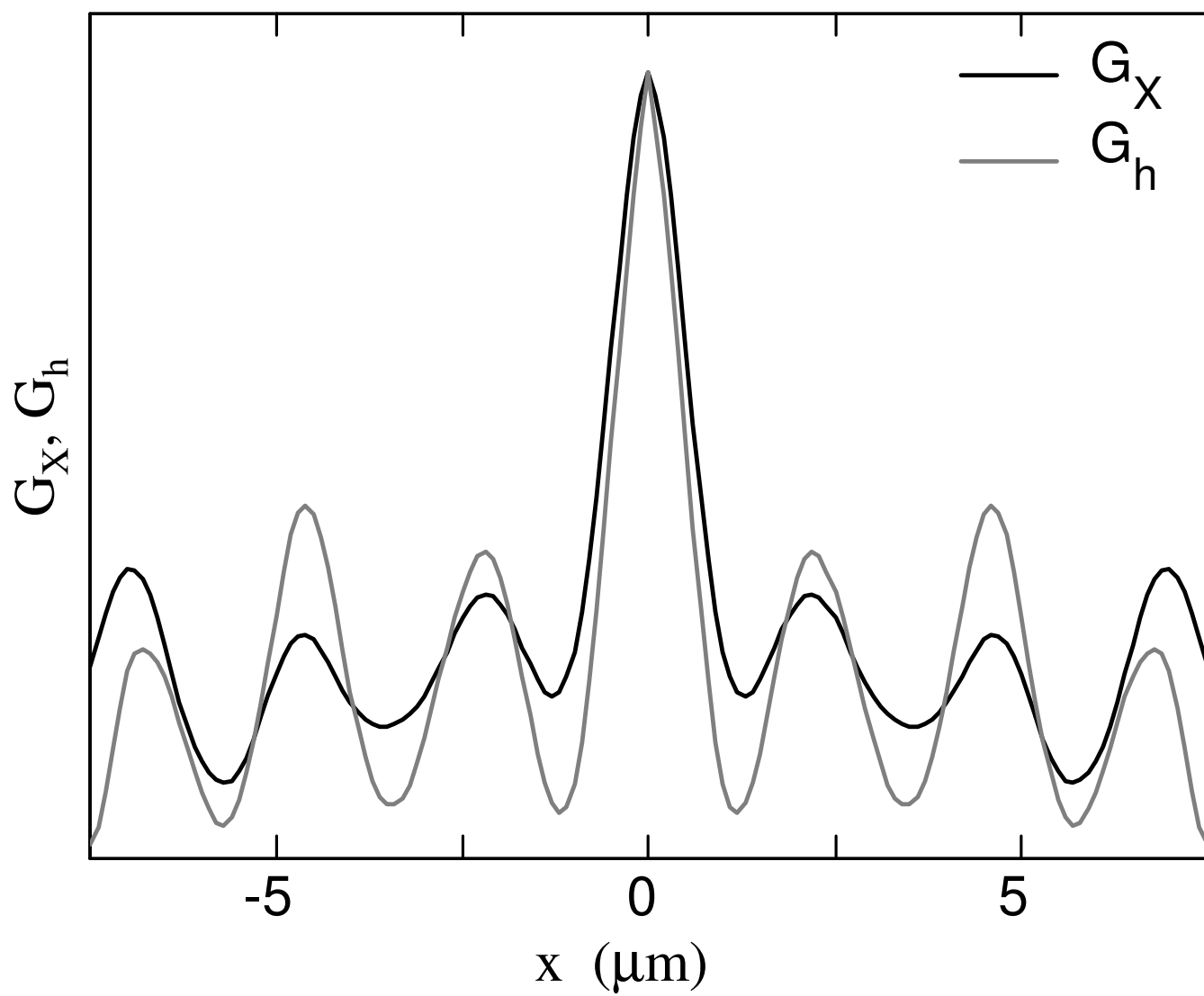


Fig. 4 Yayon et al.

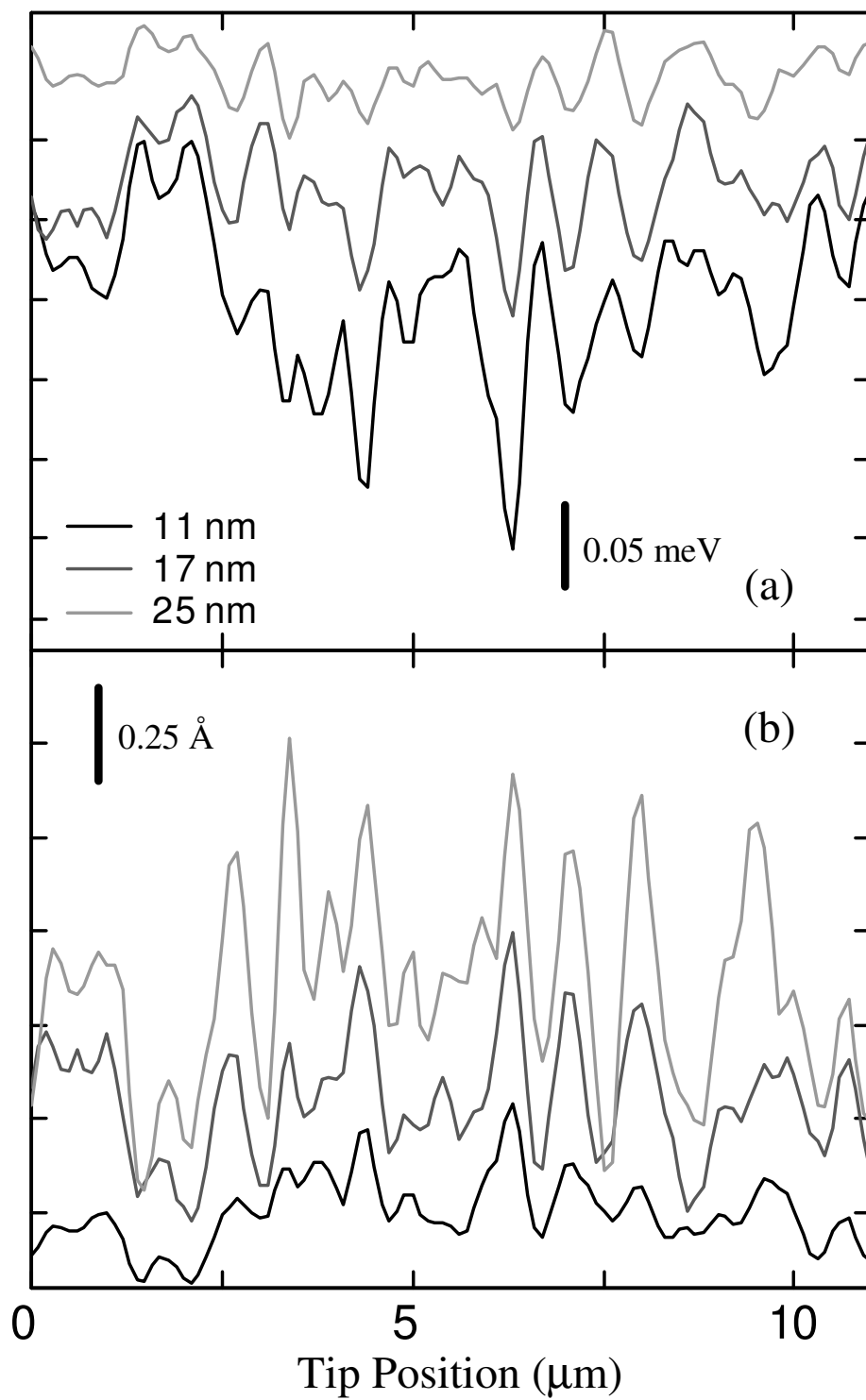


Fig. 5 Yayon et al.

